Asian Journal of Current Research in Clinical Cancer
ISSN: 3062-4444
2023, Volume 3, Issue 1, Page No: 142-158

Available online at: www.galaxypub.co/page/journals

Galaxy Publication

Galaxy Publication

Wnt/β-Catenin–Driven miR-23a/27a/24-2 Cluster Sustains Immune Escape and Immunotherapy Resistance in NSCLC

Camila Sato[1]*, Mei T. Taylor[1], Daniel Martinez[1]

[1]Department of Clinical Cancer Research, Faculty of Medicine, Heidelberg University, Heidelberg, Germany.

***E-mail** ✉ csato@gmail.com

Received: 24 April 2023; **Revised:** 04 August 2023; **Accepted:** 09 August 2023

ABSTRACT

Programmed cell death ligand 1 (PD-L1) and major histocompatibility complex class I (MHC-I) serve as crucial mediators in tumor immune escape mechanisms and in conferring resistance to PD-1/PD-L1 checkpoint inhibition. In this study, we found that elevated expression of every miRNA within the miR-23a/27a/24−2 cluster was linked to worse patient outcomes, enhanced immune evasion, and reduced response to PD-1/PD-L1 therapy in non-small cell lung cancer (NSCLC) cases. Increased levels of these cluster miRNAs promoted PD-L1 upregulation via direct suppression of Cbl proto-oncogene B (CBLB) and led to MHC-I downregulation by boosting eukaryotic translation initiation factor 3B (eIF3B) through inhibition of microphthalmia-associated transcription factor (MITF). We further showed that sustained expression of the miR-23a/27a/24−2 cluster in NSCLC relies on augmented Wnt/β-catenin pathway activity, which enhances binding of transcription factor 4 (TCF4) to the cluster's promoter region. Importantly, therapeutic inhibition of the eIF3B axis markedly improved responsiveness to PD-1/PD-L1 blockade in NSCLC tumors with strong miR-23a/27a/24−2 cluster activity. This improvement stemmed from restored MHC-I levels without diminishing the cluster-driven high PD-L1 status. Collectively, our findings delineate how these cluster miRNAs perpetuate their own transcription and elucidate the pathways through which they facilitate tumor immune avoidance and therapy resistance to PD-1/PD-L1 inhibitors. Moreover, we introduce an innovative treatment modality for NSCLC characterized by robust miR-23a/27a/24−2 cluster expression.

Keywords: NSCLC, Immunotherapy resistance, Cluster, Immune

How to Cite This Article: Sato C, Taylor MT, Martinez D. Wnt/β-Catenin–Driven miR-23a/27a/24-2 Cluster Sustains Immune Escape and Immunotherapy Resistance in NSCLC. Asian J Curr Res Clin Cancer. 2023;3(1):142-58. https://doi.org/10.51847/hLdMPyjEtk

Introduction

Lung cancer remains the most frequent malignant disease and the top cause of cancer-related deaths across the globe [1]. Among its subtypes, non-small cell lung cancer (NSCLC) predominates, representing 85% of total lung cancer diagnoses [2]. Even with recent therapeutic advances, survival rates for NSCLC remain poor, as fewer than 20% of patients live beyond 5 years [2, 3]. Growing research highlights immune escape as a central driver of tumor progression and a key impediment to successful cancer treatments [4]. As a result, immune-based strategies, particularly immune checkpoint inhibitors (ICB), have gained prominence in managing multiple malignancies, including NSCLC, with notable clinical successes reported [3, 5]. Yet, whether used singly or alongside chemotherapy, these agents provide lasting benefits to only a fraction of patients [3, 6]. Thus, gaining deeper insight into the processes underlying tumor immune evasion and ICB non-response is essential for designing next-generation interventions.

Various regulators, including microRNAs (miRNAs), play roles in orchestrating tumor immune avoidance. Of particular interest, miRNA clusters often act in concert to influence immune escape, with individual members targeting the same or related genes in shared pathways [7, 8]. The miR-23a/27a/24−2 cluster comprises miR-23a, miR-27a, and miR-24-2; earlier work from our group indicated that these miRNAs are overexpressed in early

NSCLC and drive post-surgical relapse by activating Wnt/β-catenin signaling [9]. Notably, heightened Wnt/β-catenin activity has been tied to immune exclusion and poor ICB outcomes in NSCLC [10]. Other reports have also linked this cluster to reduced interferon-γ (IFN-γ) production and impaired antigen-directed killing by CD8+ T cells [11]. Given this evidence, we posited that overexpression of miR-23a/27a/24−2 cluster members might contribute to immune evasion and resistance against ICB in NSCLC.

In the present research, we confirmed that higher levels of miR-23a/27a/24−2 cluster miRNAs strongly correlated with immune escape phenotypes and lack of response to PD-1/PD-L1 inhibition in NSCLC. Results from our experiments demonstrated that these cluster miRNAs substantially reduced IFN-γ release from T lymphocytes, hindered CD8+ T cell recruitment to tumors, lowered major histocompatibility complex class I (MHC-I) levels, and increased programmed cell death ligand 1 (PD-L1) abundance in NSCLC tissues. At the molecular level, the cluster miRNAs elevated PD-L1 by repressing its inhibitor Cbl proto-oncogene B (CBLB) and diminished MHC-I by elevating eukaryotic translation initiation factor 3B (eIF3B) via blockade of its repressor, microphthalmia transcription factor (MITF), within NSCLC cells. We also discovered that these miRNAs self-maintain their transcription through Wnt/β-catenin-driven enhancement of transcription factor 4 (TCF4) recruitment to the cluster promoter. Lastly, we illustrated that drug-based blockade of either the eIF3B cascade or the β-catenin/TCF4 pathway potentiated PD-1/PD-L1 inhibitor activity in NSCLC models with elevated cluster miRNA expression. Among these, eIF3B-directed intervention proved superior in amplifying the benefits of PD-1/PD-L1 therapy.

Materials and Methods

Human specimens and cell maintenance

Peripheral blood samples were drawn from 20 healthy individuals to obtain peripheral blood mononuclear cells (PBMCs). Tumor samples from non-small cell lung cancer (NSCLC) were harvested from 82 patients via surgical procedures or biopsies at Daping Hospital, in compliance with protocols approved by the relevant ethics boards. Every cell line utilized here was sourced from the Shanghai Cell Bank, Chinese Academy of Sciences (Shanghai, China). Both 293T and Lewis lung carcinoma (LLC) lines were propagated in Dulbecco's modified Eagle's medium enriched with 10% fetal bovine serum (FBS) (HyClone, Logan, UT). The H1299 and H1650 lines were maintained in RPMI1640 medium containing 10% FBS.

Plasmids and vectors

Plasmids encoding MITF (EX-B5124-M35), CBLB (EX-Z7996-M35), and eIF3B-targeting shRNA (HSH066232), together with matching control (empty or scrambled) vectors, were acquired from iGene Biotechnology Co., Ltd. (Guangzhou, China). A β-catenin overexpression vector (HG11279-CF) was purchased from Sino Biological Inc. (Beijing, China). Vectors for overexpression of the miR-23a/27a/24−2 cluster, along with shRNA and scrambled controls, were supplied by Genechem Co. Ltd. (Shanghai, China). To generate miRNA target reporters, the 3′-untranslated regions (3′-UTRs) of CBLB and MITF were PCR-amplified from cDNA prepared from healthy human lung RNA and ligated into the MluI/HindIII sites of the pMIR-REPORT™ luciferase vector (Thermo Fisher Scientific, Waltham, MA, USA). For cluster promoter reporters, the miR-23a/27a/24−2 promoter fragment was amplified from human genomic DNA and subcloned into the NheI/BglII sites of the pGL4.10 luciferase vector (Promega, Madison, WI, USA).

T cell–tumor cell coculture experiments

PBMCs were purified from fresh donor blood using lymphocyte separation medium per the supplier's directions (Tian Jin Hao Yang Biological Manufacture Co., Ltd, Tianjin, China). T cells were activated following previously published methods [12]. Pure CD8+ T cells were then isolated with a CD8+ T cell isolation kit (Miltenyi Biotec) as recommended by the manufacturer.

Cytotoxicity mediated by T cells was quantified according to an established procedure [12]. NSCLC cells were first transfected with control or miR-23a/27a/24−2 cluster overexpression vectors. At 48 hours post-transfection, the tumor cells were incubated with activated T cells (1:20 ratio) for 6 hours, followed by assessment of tumor cell death via flow cytometry.

CD8+ T cell chemotaxis was tested using the approach detailed by Shang *et al*. [13]. Transfected NSCLC cells (control or cluster-overexpressing) received fresh medium 48 hours after transfection. After another 48 hours,

conditioned medium was placed in the lower Transwell chamber. Activated CD8+ T cells (5 × 10^5 cells in 100 μl), stained with anti-human CD8α APC-Cy7 antibody (Invitrogen, Cat#: A15448), were seeded in the upper chamber. Migrated cells were counted by flow cytometry after 2 hours.
The influence of cluster-overexpressing NSCLC cells on T cell IFN-γ production was evaluated by coculturing transfected tumor cells with activated T cells (1:10 ratio) for 12 hours. Supernatants were collected, and IFN-γ levels were determined with a human IFN-γ ELISA kit (Invitrogen) following the provided protocol.

Luciferase reporter experiments
For validation of miRNA targets, 293T cells carrying firefly luciferase reporters with CBLB or MITF 3′-UTRs were cotransfected with miR-23a/27a/24−2 cluster vectors or controls. For promoter activity studies, 293T cells harboring the cluster promoter luciferase reporter were cotransfected with TCF4, β-catenin, or control plasmids. Renilla luciferase vector served as normalization control. Cells were collected 72 hours later, and luciferase signals were recorded using the Dual-Luciferase Assay System (Promega).

Western blotting (WB), immunohistochemistry (IHC), immunofluorescence (IF), and co-immunoprecipitation (Co-IP)
These assays were carried out as reported earlier [14]. WB signals were densitometrically analyzed with ImageJ. IHC slides were scored blindly by two pathologists unfamiliar with patient data. Primary antibodies used were: anti-eIF3B (Cat No: bs-14542R, Lot No: BC12254757; IHC), anti-MITF (Cat No: bsm-51339 M, Lot No: BD06051693), anti-MHC-I (Cat No: bs-18070R, Lot No: BD07151765, WB; bs-2355R, Lot No: BD07151765, IHC/IF), and anti-PD-L1 (Cat No: bs-22022R, Lot No: BD7153735, flow cytometry) from Beijing Biosynthesis Biotechnology Co., Ltd (Beijing, China); anti-β-catenin (Cat No: 8480 S, Lot No: 5), anti-Histone H3 (Cat No: 9715 S, Lot No: 20), and anti-Actin (Cat No: 4970 S, Lot No: 20) from Cell Signaling Technology (Danvers, MA, USA); anti-CD8 (Cat No: ab217344, Lot No: 00121531; ab17147, Lot No: 3258634-5) and anti-PD-L1 (Cat No: ab279292, Lot No: 1007824-2, WB) from Abcam (Cambridge, MA, USA); anti-CBLB (Cat No: 66353-1, Lot No: 10003654), anti-TCF4 (Cat No: 22337-1-AP, Lot No: 00121531), anti-eIF3B (Cat No: 68202-1, Lot No: 10028876, WB), and anti-PD-L1 (Cat No: 66248-1, Lot No: 10022147, IHC) from Proteintech (Wuhan, Hubei, China). Control rabbit IgG (Cat No: 30000-0-AP, Lot No: 00140749) and mouse IgG (Cat No: BS-0296P, Lot No: BC06261797) came from Proteintech and Beijing Biosynthesis Biotechnology Co., Ltd, respectively.

Quantitative real-time PCR (qRT-PCR) and miRNA in situ hybridization (ISH)
Total RNA was prepared with TRIzol reagent (Beyotime, Shanghai, China). mRNA quantification was performed via qRT-PCR using the SYBR Green One-Step kit (Beyotime Biotechnology) as directed. Primers for U6, hsa-miR-23a, hsa-miR-24-2, and hsa-miR-27a were obtained from GeneCopoeia (Rockville, MD, USA), with detection carried out using the All-in-One™ miRNA qRT-PCR Detection Kit 2.0 (GeneCopoeia). miRNA levels were normalized against U6.
ISH for miRNAs followed the protocol of Nuovo [15], and scoring was based on Guo *et al*. [16]. Paraffin sections were deparaffinized, antigen-retrieved by 15-minute boiling in citric acid buffer, treated with proteinase K for 15 minutes, and pre-hybridized at 37°C for 1 hour. Overnight hybridization at 37°C was performed with probes specific for miR-23a, miR-24-2, or miR-27a (or no probe as negative control). Probes were custom-made by Zoonbio Biotechnology Co., Ltd (Nanjing, China).

RNA sequencing and proteomics analysis
Transcriptome sequencing and subsequent analysis were carried out by Shanghai Genechem Co., Ltd., following the protocol outlined by Li *et al*. [17]. In brief, Illumina RNA libraries were prepared using the NEBNext Ultra RNA library prep kit and sequenced on the Illumina NovaSeq platform. Raw FASTQ data were processed with custom in-house Perl scripts, and Hisat2 was employed as the alignment tool to generate a splice junction database based on the provided gene model annotation file.
Proteomics studies were conducted as reported earlier [18]. In short, H1299 cells were transfected with either the miR-23a/27a/24−2 cluster overexpression vector or control plasmid. Seventy-two hours later, cellular proteins were harvested, denatured, digested, and tagged with iTRAQ reagents. The tagged peptides were separated using an Agilent 1260 Infinity II HPLC system. Mass spectrometry was performed on a Q-Exactive Plus instrument

(Thermo Fisher Scientific) interfaced with an Easy-nLC system (Thermo Fisher Scientific). Data processing was done with Mascot 2.6 and Proteome Discoverer 2.1 software.

Electrophoretic mobility shift assay (EMSA)

Potential TCF4 binding sites within the miR-23a/27a/24−2 cluster were identified using the hTFtarget database [19]. EMSA experiments were executed with the LightShift Chemiluminescent EMSA Kit (Thermo Fisher Scientific) per the manufacturer's guidelines and as detailed previously [14].

Chromatin immunoprecipitation (ChIP)-qPCR assay

For ChIP-qPCR experiments, 293T cells were transfected with a β-catenin expression plasmid or empty vector. Forty-eight hours post-transfection, cells were fixed with 1% formaldehyde at room temperature, and the reaction was quenched by adding glycine. Cells were then lysed in ChIP lysis buffer, sheared by sonication, precleared, and incubated overnight with 2 μg of anti-TCF4 antibody or control IgG, followed by precipitation using protein G/A beads. Beads were washed sequentially with low- and high-salt buffers, and bound chromatin was eluted at 65°C for 15 minutes. After centrifugation to recover the supernatant, NaCl was added (final concentration 0.2 M), and samples were incubated overnight at 65°C to reverse crosslinks. DNA was purified and analyzed by qPCR.

Animal study

Six-week-old female C57BL/6J mice and male SCID mice (Beijing HFK Bioscience Co., Ltd, Beijing, China) were employed for in vivo experiments. The role of the miR-23a/27a/24−2 cluster in lung cancer immune escape was assessed in C57BL/6J and SCID xenograft models. To establish C57BL/6J xenografts, 1 × 10^6 LLC cells transfected with control vector, miR-23a/27a/24−2 cluster overexpression plasmid, scrambled control, or cluster-specific shRNA were suspended in 100 μl PBS and injected subcutaneously into the flanks of mice. For SCID xenografts, 2 × 10^6 H1299 cells transfected with scrambled control or cluster shRNA plasmid were injected subcutaneously in 100 μl PBS. Three days after tumor cell implantation, mice received either no treatment or 3 × 10^6 human PBMCs via tail vein injection. Tumor volumes were monitored weekly.

The contribution of the miR-23a/27a/24−2 cluster to resistance against PD-1/PD-L1 blockade was evaluated in C57BL/6J xenograft models. Mice were subcutaneously implanted with 1 × 10^6 LLC cells transfected with control vector or miR-23a/27a/24−2 cluster plasmid in 100 μl PBS. Once tumors reached approximately 100 mm^3, animals were administered PD-L1 monoclonal antibody (1 mg/kg body weight) or control rat IgG (Bio X Cell) every three days via intravenous injection.

To evaluate the combined therapeutic impact of LF3 and PD-1/PD-L1 blockade in tumors with elevated miR-23a/27a/24−2 cluster expression, C57BL/6J xenografts were established using cluster-overexpressing LLC cells as described. When tumors attained ~100 mm^3, mice were randomized into four groups: control (IgG), PD-L1 mAb alone (1 mg/kg every three days), LF3 alone (50 mg/kg every two days), or PD-L1 mAb plus LF3, all via intravenous injection.

To assess the relative benefits of LF3 versus 4EGI-1 when combined with PD-1/PD-L1 blockade, C57BL/6J xenografts were created with cluster-high LLC cells. At ~100 mm^3 tumor volume, mice were divided into three groups: PD-L1 mAb alone (1 mg/kg every three days), PD-L1 mAb plus LF3, or PD-L1 mAb plus 4EGI-1 (75 mg/kg, intraperitoneal, 5 days/week). All animal procedures adhered to the Army Medical University guidelines on laboratory animal care and use.

Statistical analysis

Results are expressed as mean ± standard deviation from at least three independent replicates. Statistical comparisons were performed using SPSS software, with differences deemed significant when $p < 0.05$.

Results and Discussion

Elevated levels of miRNAs from the miR-23a/27a/24−2 cluster are closely linked to disease advancement and immune escape in NSCLC

To explore the relationship between miR-23a/27a/24−2 cluster miRNA levels and NSCLC progression, patients were categorized based on tumor versus adjacent tissue expression. Those showing higher levels of all cluster miRNAs in tumors were assigned to the high-expression group, while those with lower or comparable levels were

placed in the low-expression group. Clinical findings indicated that miR-23a/27a/24−2 cluster expression inversely correlated with overall survival **(Figure 1a)** and disease-free survival **(Figure 1b)** in NSCLC cases. Moreover, the high-expression group exhibited reduced CD8+ T cell infiltration within tumor sites **(Figure 1c).** Gene Ontology (GO) enrichment from transcriptome sequencing of miR-23a/27a/24−2 cluster-knockdown H1299 cells versus controls highlighted impacts on T cell activation and differentiation **(Figure 1d).** Gene set enrichment analysis (GSEA) further demonstrated a negative association between cluster miRNA levels and T cell-mediated immunity in NSCLC **(Figure 1e).** Similar patterns emerged from GEO dataset examination, where cluster expression correlated with altered T cell activation and differentiation **(Figure 1f).** Additionally, target prediction-based functional assessment of the cluster miRNAs pointed to involvement in immune-related processes [20] **(Figure 1g).** Collectively, these observations imply that increased miR-23a/27a/24−2 cluster miRNAs drive NSCLC progression through suppression of T cell-mediated immunity.

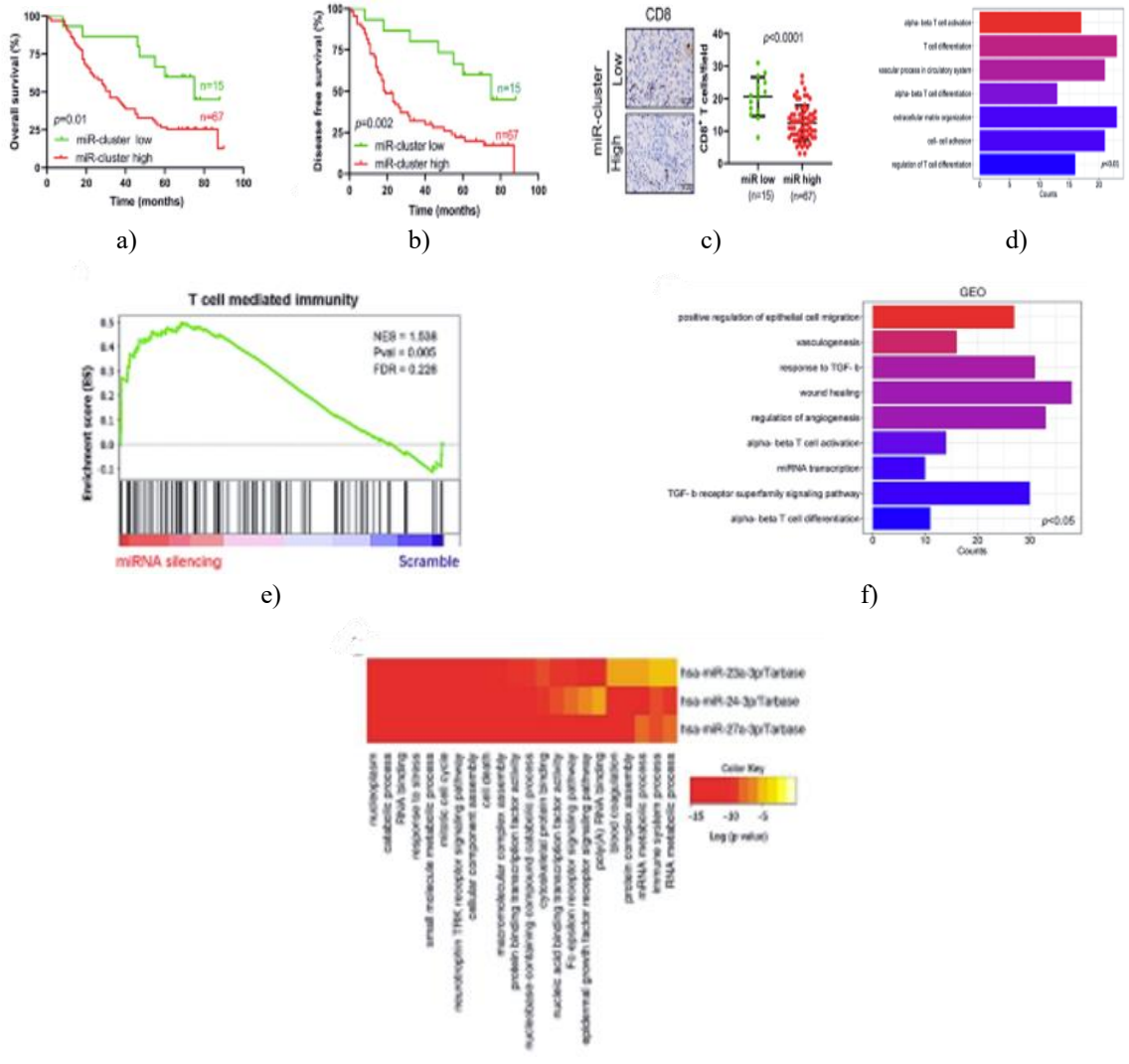

Figure 1. Elevated miR-23a/27a/24−2 cluster expression strongly associates with unfavorable outcomes and immune evasion in NSCLC tumors. (a) Kaplan-Meier curves illustrating reduced overall survival and (b) reduced disease-free survival in NSCLC patients with high cluster expression. Analyses involved 82 patients, with log-rank tests for significance. (c) Representative IHC stainingfor CD8+ T cells and quantification of infiltration (per 100 × 100 μm field). Significance determined by t-test. (d) GO enrichment based on RNA-seq from cluster-silenced versus control H1299 cells. (e) GSEA indicating inverse correlation between cluster expression and T cell-mediated immunity, derived from RNA-seq of silenced versus control H1299 cells. (f) GO analysis using GEO dataset GSE151103. (g) Target-based GO analysis for the cluster miRNAs (via http://www.microrna.gr/miRPathv4). miR-cluster denotes miR-23a/27a/24−2 cluster.

Overexpression of the miR-23a/27a/24−2 cluster in NSCLC suppresses T cell-driven immune responses

To determine if cluster-overexpressing NSCLC cells directly impair T cell function, activated T cells were cocultured with these modified tumor cells, followed by evaluation of T cell activity. Findings showed that high cluster expression in NSCLC cells markedly decreased IFN-γ release by T cells **(Figure 2a)**, diminished T cell-induced tumor cell killing **(Figure 2b)**, and restricted T cell chemotaxis **(Figure 2c)**. The cluster's role in immune evasion was further probed in vivo using Lewis lung carcinoma (LLC) models. Since LLC tumors develop in immunocompetent C57BL/6J mice, this system suits immunity studies [21]. In C57BL/6J xenografts, overexpressing all cluster miRNAs in LLC cells accelerated tumor growth **(Figure 2d)**, reduced CD8+ T cell tumor infiltration **(Figure 2e),** and lowered T cell IFN-γ production **(Figure 2f).** Conversely, cluster knockdown in LLC cells slowed tumor expansion **(Figure 2g)**, enhanced CD8+ T cell presence **(Figure 2h),** and boosted IFN-γ levels **(Figure 2i).** These effects were validated in additional models. Cluster silencing in H1299 cells substantially curtailed tumor growth in SCID mice, both with **(Figure 2j)** and without **(Figure 2l)** PBMC transfer. In PBMC-treated SCID models, cluster inhibition also increased T cell infiltration **(Figure 2k).** Strikingly, PBMC administration amplified the growth-suppressive impact of cluster silencing **(Figure 2m).** Overall, these results highlight the miR-23a/27a/24−2 cluster's contribution to dampening antitumor T cell responses.

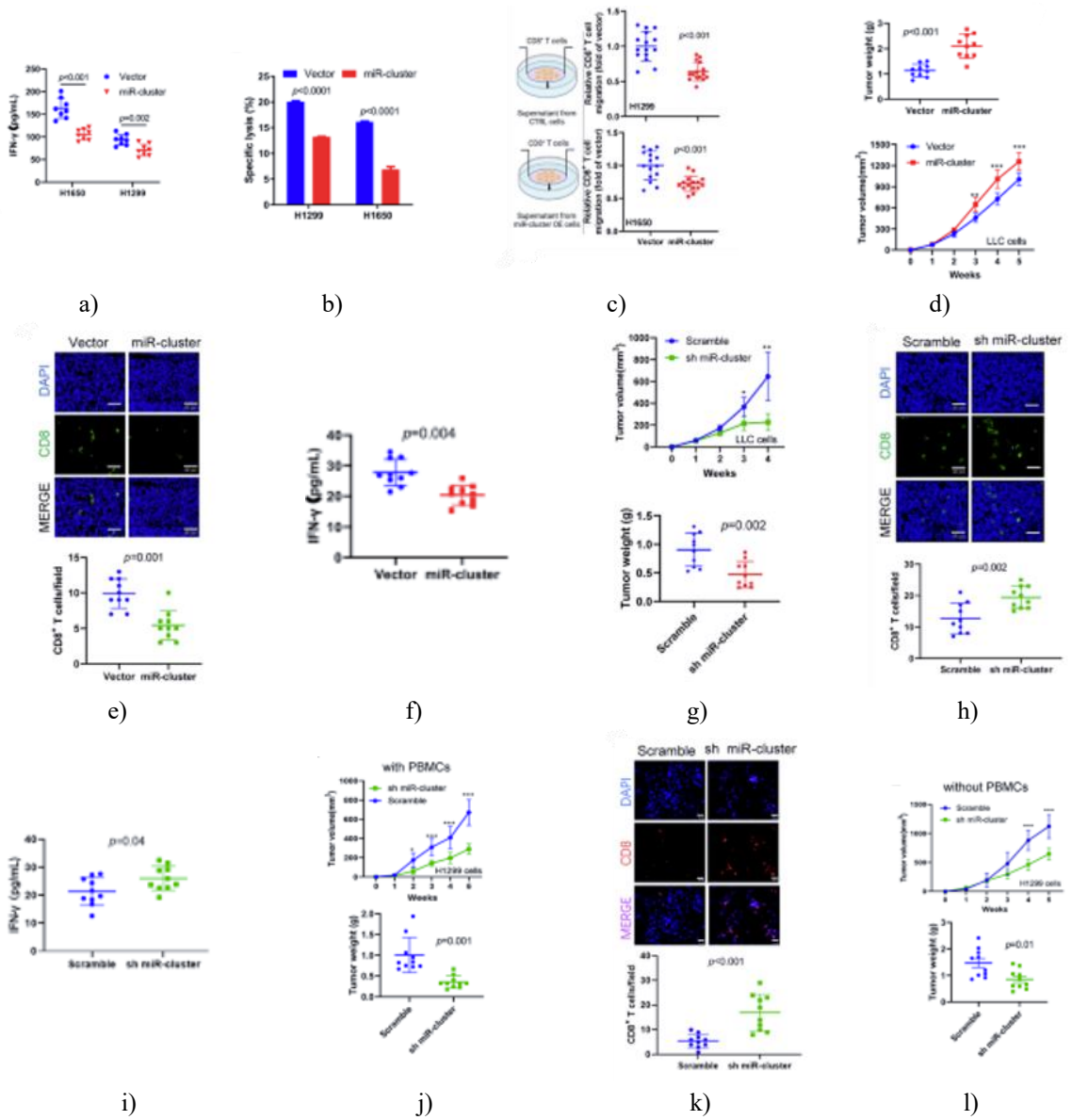

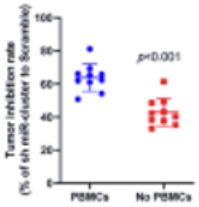

m)

Figure 2. The miR-23a/27a/24−2 cluster suppresses T cell-mediated antitumor immunity in NSCLC. (a) IFN-γ levels in culture supernatants following 12-hour coculture of CD8+ T cells with NSCLC cells at a 10:1 ratio. (b) Flow cytometric measurement of CD8+ T cell-mediated killing of NSCLC cells. Transfected NSCLC cells (vector or miR-23a/27a/24−2 cluster) were cocultured with activated CD8+ T cells at a 1:20 ratio for 6 hours. (c) Relative chemotaxis of human CD8+ T cells toward conditioned medium from H1299 or H1650 cells transfected with control or cluster-overexpression vectors. (d) Tumor growth curves and final weights in subcutaneous C57BL/6J xenografts established with LLC cells transfected with control or miR-23a/27a/24−2 cluster vectors. (e) Representative immunofluorescence staining for CD8+ T cells (green) and quantification of infiltration (per 100 × 100 μm field) in tumors from (d) (scale bar: 50 μm). (f) IFN-γ concentrations in tumor lysates from the C57BL/6J xenografts in (d). (g) Tumor growth curves and weights in C57BL/6J xenografts using LLC cells transfected with scrambled control or miR-23a/27a/24−2 cluster shRNA. (h) Representative immunofluorescence for CD8+ T cells (green) and infiltration counts (per 100 × 100 μm field) in tumors from (g) (scale bar: 50 μm). (I) IFN-γ levels in tumor lysates from xenografts in (g). (j) Tumor growth and weights in PBMC-treated SCID xenografts established with H1299 cells transfected with scrambled or cluster shRNA vectors. (k) Representative immunofluorescence for CD8+ T cells (red) and infiltration quantification (per 100 × 100 μm field) in tumors from (j) (scale bar: 50 μm). (l) Tumor growth and weights in SCID xenografts without PBMC treatment, using the same H1299 transfectants as in (j). (m) Tumor growth inhibition rates upon cluster silencing in SCID models with or without PBMC administration, based on data from (j) and (l). Animal studies included 10 mice per group. In vitro assays were performed in triplicate. Data represent mean ± SD. Significance assessed by t-test: *, $p < 0.05$; , $p < 0.01$; *, $p < 0.001$ versus vector or scramble control. LLC, Lewis lung cancer; IFN-γ, interferon-γ; miR-cluster, miR-23a/27a/24−2 cluster; sh miR-cluster, shRNA targeting miR-23a/27a/24−2 cluster; PBMCs, peripheral blood mononuclear cells.

miRNAs from the miR-23a/27a/24−2 cluster elevate PD-L1 while reducing MHC-I levels in NSCLC

To identify proteins mediating the immunosuppressive actions of the miR-23a/27a/24−2 cluster miRNAs on T cell responses, we conducted proteomic profiling in NSCLC cells overexpressing the entire cluster versus controls. Results demonstrated that cluster overexpression altered numerous proteins, notably increasing PD-L1 and decreasing MHC-I—both critical for immune escape and resistance to immune checkpoint blockade **(Figure 3a).** Gene Ontology analysis further linked cluster overexpression to pathways involving MHC-I antigen processing and presentation **(Figure 3a).** Western blotting confirmed that the cluster enhanced PD-L1 while suppressing MHC-I expression in NSCLC cells, irrespective of IFN-γ stimulation **(Figure 3b)**. This indicates direct regulation of PD-L1 and MHC-I by the cluster, independent of its effects on T cell IFN-γ production. Co-overexpression of all cluster miRNAs exerted stronger modulation of PD-L1 and MHC-I than individual miRNAs, revealing synergistic activity. These changes were validated by flow cytometry **(Figure 3c)** and immunofluorescence **(Figure 3d).** Proteomics data aligned with these observations. Immunohistochemistry in LLC-based C57BL/6J xenografts showed elevated PD-L1 and reduced MHC-I in cluster-overexpressing tumors **(Figure 3e).** Similar patterns emerged in human NSCLC specimens, with high-cluster patients displaying higher PD-L1 and lower MHC-I **(Figure 3f).** Overall, these findings indicate that the miR-23a/27a/24−2 cluster impairs T cell antitumor immunity by boosting PD-L1 and diminishing MHC-I expression in NSCLC.

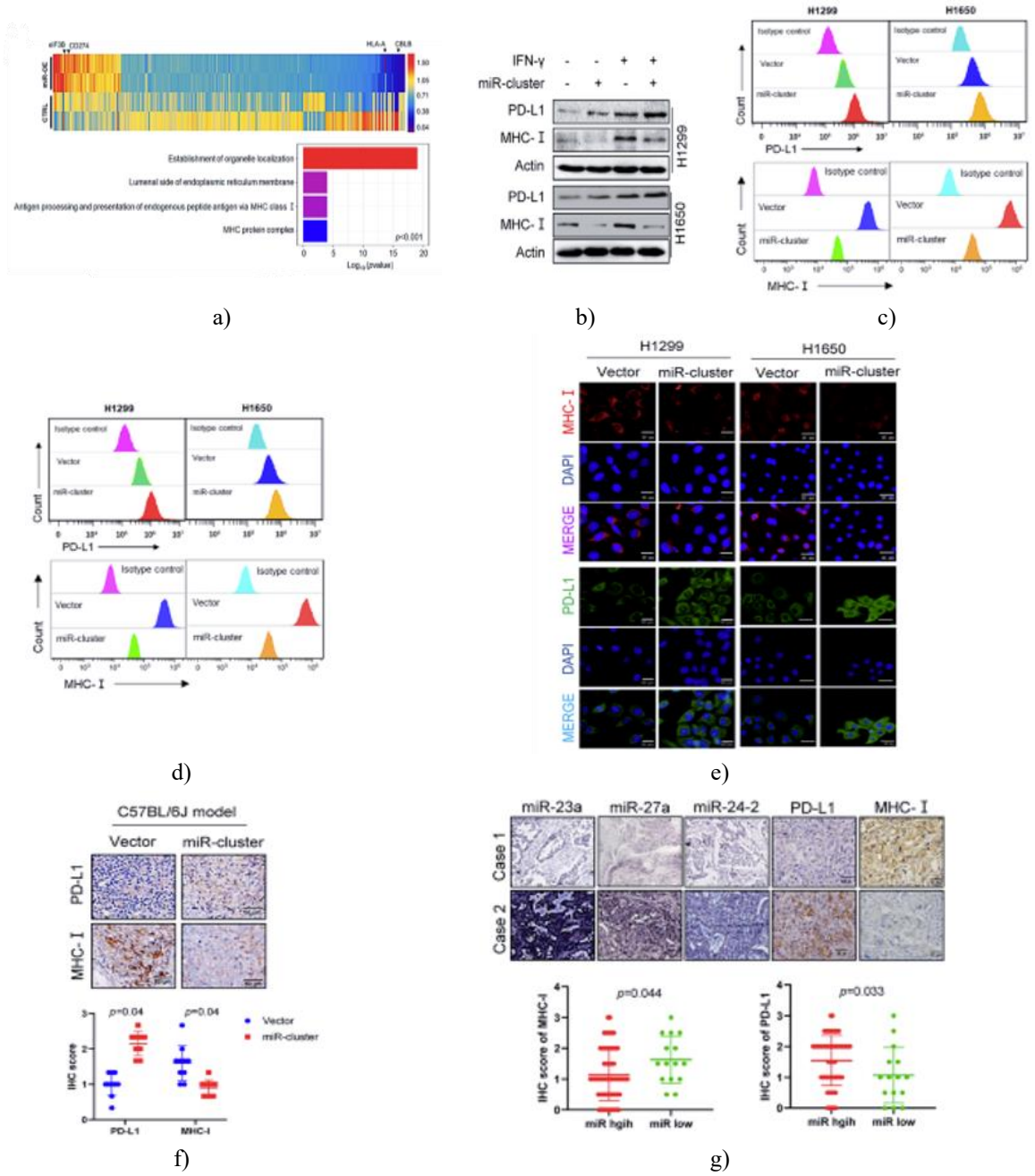

Figure 3. The miR-23a/27a/24−2 cluster modulates PD-L1 and MHC-I levels in NSCLC. (a) Heatmap of differentially expressed proteins and Gene Ontology enrichment from proteomics in cluster-overexpressing versus control H1299 cells. (b) Western blots demonstrating cluster-mediated upregulation of PD-L1 and downregulation of MHC-I in NSCLC cells, with or without 20 ng/ml IFN-γ treatment (24 hours). (c) Flow cytometry and (d) immunofluorescence (scale bar: 20 μm) confirming reduced MHC-I and increased PD-L1 upon cluster overexpression. Cells were analyzed 72 hours post-transfection with control or cluster vectors (b-d). Assays performed in triplicate. (e) Representative IHC staining and scoring for PD-L1 and MHC-I in C57BL/6J xenografts from **Figure 2d** (scale bar: 50 μm). (f) IHC images and scores for PD-L1 and MHC-I in human NSCLC tissues from patients with high (n = 67) or low (n = 15) cluster expression (scale bar: 50 μm). Significance by Wilcoxon signed-rank test (e) or Wilcoxon rank-sum test (f). miR-cluster, miR-23a/27a/24−2 cluster; miR-OE, cluster overexpression; CTRL, control; miR high, high cluster miRNA expression; miR low, low cluster miRNA expression.

miRNAs from the miR-23a/27a/24−2 cluster enhance PD-L1 expression in NSCLC via targeting CBLB

We next explored how the miR-23a/27a/24−2 cluster miRNAs control PD-L1 levels in NSCLC. Proteomics data showed reduced CBLB in cells overexpressing the cluster **(Figure 3a);** CBLB acts as a known negative regulator

of PD-L1 in NSCLC [22]. Western blotting and qRT-PCR confirmed that cluster miRNAs suppressed CBLB at both protein **(Figure 4a),** and mRNA levels **(Figure 4b).** Crucially, restoring CBLB expression blocked the cluster-driven increase in PD-L1 **(Figure 4c)**, indicating that the cluster elevates PD-L1 by repressing CBLB. Bioinformatic prediction (targetscan.org) identified binding sites for miR-23a and miR-27a in the CBLB 3′-untranslated region (3′-UTR) **(Figure 4d).** Luciferase reporter assays demonstrated that cluster overexpression markedly reduced activity from the wild-type CBLB 3′-UTR reporter but had no effect on the mutated version **(Figure 4e).** Inverse correlation between the cluster and CBLB, alongside positive correlation with PD-L1, was validated by IHC in tumors from cluster-overexpressing LLC-based C57BL/6J xenografts **(Figure 4f)** and human NSCLC samples **(Figure 4g).** Overall, these results establish that miR-23a/27a/24−2 cluster miRNAs boost PD-L1 expression in NSCLC by directly suppressing CBLB through 3′-UTR targeting.

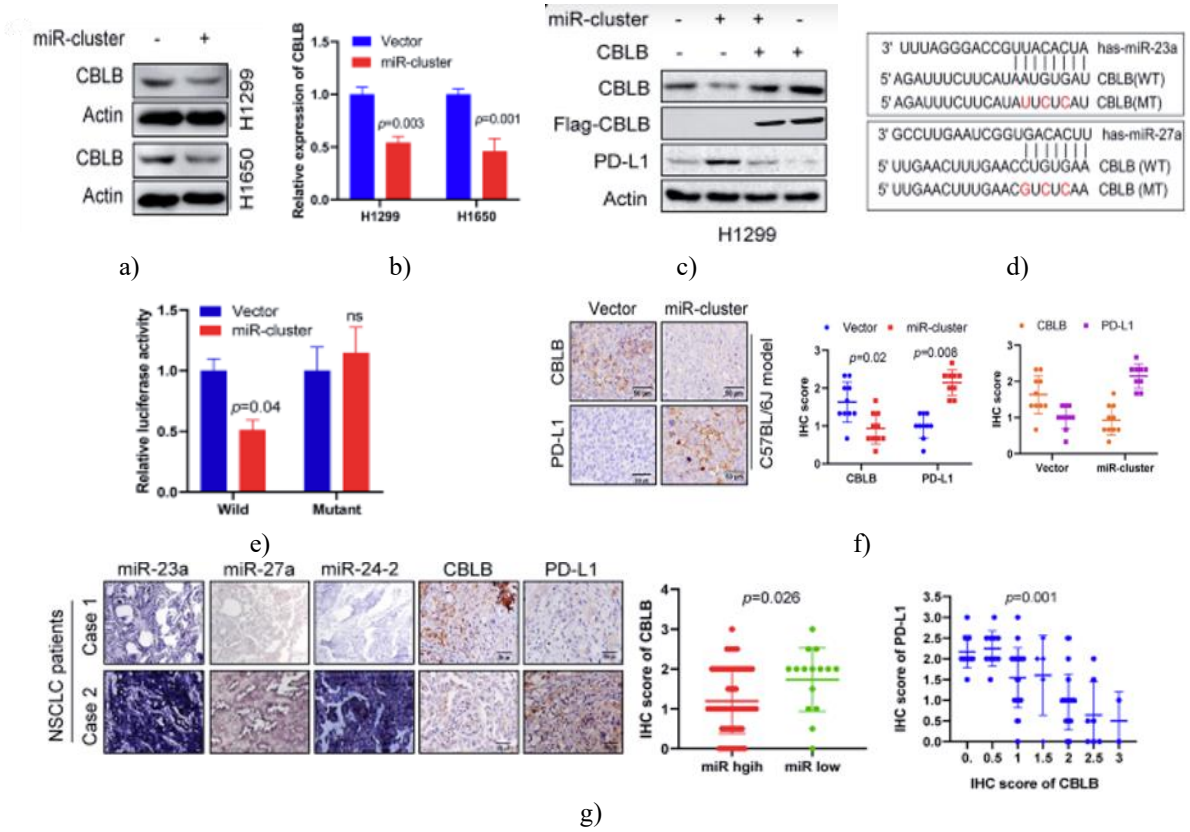

Figure 4. The miR-23a/27a/24−2 cluster promotes PD-L1 expression through CBLB suppression in NSCLC. (a) Western blot and (b) qRT-PCR demonstrating cluster overexpression reduces CBLB at protein and mRNA levels. (c) CBLB restoration prevents cluster-mediated PD-L1 upregulation in H1299 cells. NSCLC cells were transfected with control vector, cluster overexpression construct, and/or CBLB construct; analyses performed 72 hours later. Assays repeated in triplicate (a-c). (d) Alignment of cluster miRNAs with CBLB 3′-UTR binding sites. (e) Luciferase reporter assay showing cluster overexpression inhibits wild-type but not mutant CBLB 3′-UTR-driven luciferase activity. (f) Representative IHC staining and scores for CBLB and PD-L1 in C57BL/6J xenograft tumors from **Figure 2d** (scale bar: 50 μm). (g) IHC images and scores for CBLB and PD-L1 in NSCLC patient tumors with high (n = 67) or low (n = 15) cluster expression (scale bar: 50 μm). Data are mean ± SD. Significance by t-test (b, e), Wilcoxon signed-rank test (f), Wilcoxon rank-sum test (g-left), or one-way ANOVA (G-right). miR-cluster, miR-23a/27a/24−2 cluster; miR high, high cluster miRNA expression; miR low, low cluster miRNA expression.

miRNAs from the miR-23a/27a/24−2 cluster reduce MHC-I expression in NSCLC via MITF targeting

We further examined the mechanism by which the miR-23a/27a/24−2 cluster regulates MHC-I. Proteomics indicated elevated eIF3B upon cluster overexpression **(Figure 3a).** Predictive algorithms revealed potential binding sites for all three cluster miRNAs in the MITF 3′-UTR **(Figure 5a).** Prior work shows MITF suppresses eIF3B, while eIF3B in turn inhibits MHC-I [23], raising the possibility that the cluster downregulates MHC-I by

increasing eIF3B through MITF repression. In agreement, cluster overexpression in NSCLC cells strongly decreased MITF and MHC-I while raising eIF3B **(Figure 5b)**. Cluster-mediated MITF reduction was also evident at the mRNA level **(Figure 5c).** Restoring MITF or knocking down eIF3B rescued MHC-I levels diminished by the cluster **(Figure 5d)**, and MITF overexpression prevented cluster-induced eIF3B elevation **(Figure 5d).** Luciferase assays confirmed direct targeting: cluster overexpression lowered activity from the wild-type MITF 3′-UTR reporter but not the mutant **(Figure 5e).** Relationships among cluster expression, MITF, eIF3B, and MHC-I were corroborated by IHC in cluster-overexpressing LLC xenografts from C57BL/6J mice **(Figure 5f)** and human NSCLC tissues **(Figure 5g).** In summary, these data demonstrate that miR-23a/27a/24−2 cluster miRNAs suppress MHC-I in NSCLC by directly targeting MITF, thereby upregulating eIF3B.

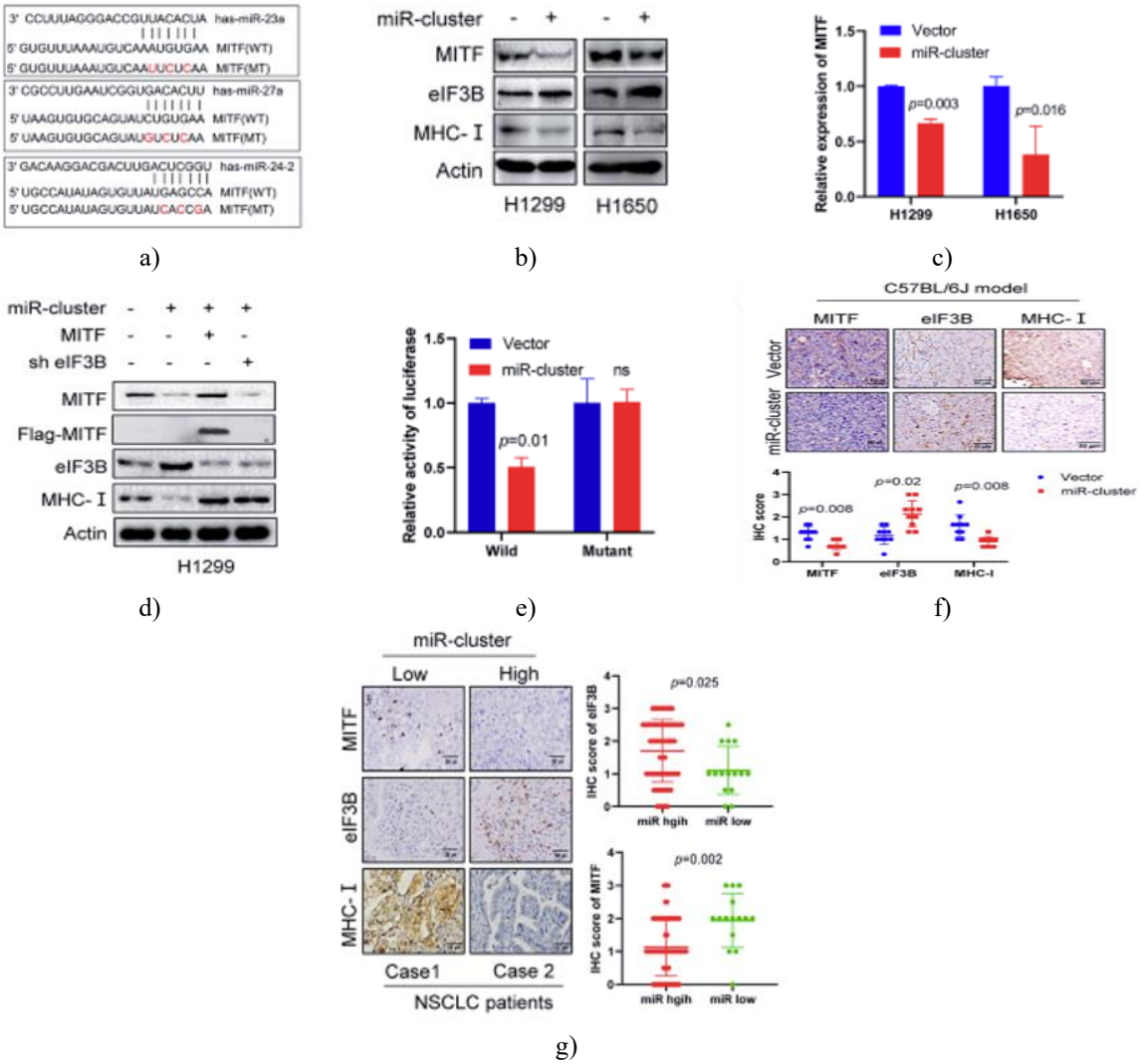

Figure 5 . The miR-23a/27a/24−2 cluster reduces MHC-I expression via the MITF/eIF3B pathway in NSCLC. (a) Alignment of cluster miRNAs with the 3′-UTR of MITF. (b) Western blot demonstrating that cluster overexpression suppresses MITF and MHC-I while increasing eIF3B in NSCLC cells. (c) qRT-PCR showing cluster overexpression inhibits MITF mRNA levels in NSCLC cells. (d) Western blot indicating that cluster-mediated MHC-I downregulation is reversed by MITF restoration or eIF3B knockdown in H1299 cells. NSCLC cells were transfected with the specified constructs and analyzed 72 hours later. Assays were performed in triplicate (b-d). (e) Luciferase reporter assay revealing that cluster overexpression inhibits wild-type MITF 3′-UTR-driven luciferase activity but not mutant versions in NSCLC cells. (f) Representative IHC staining and scores for MITF, eIF3B, and MHC-I in C57BL/6J xenograft tumors from **Figure 2d** (scale bar: 50 μm). (g) Representative IHC images and scores for MITF, eIF3B, and MHC-I in NSCLC patient tumors with high (n = 67) or low (n = 15) cluster expression (scale bar: 50 μm). Data represent mean ± SD. Significance determined by t-test (c and d), Wilcoxon signed-rank test (f), or Wilcoxon rank-sum test (g).

miR-cluster, miR-23a/27a/24−2 cluster; miR high, high cluster miRNA expression; miR low, low cluster miRNA expression.

miRNAs from the miR-23a/27a/24−2 cluster sustain their own expression via the β-catenin/TCF4 pathway in NSCLC

To elucidate how the miR-23a/27a/24−2 cluster miRNAs are regulated in NSCLC, we identified potential transcription factors and determined that TCF4 binds the cluster promoter **(Figure 6a).** TCF4, a downstream effector of Wnt/β-catenin signaling, controls miRNA transcription by engaging promoter regions [24]. Our earlier work showed that these cluster miRNAs activate Wnt/β-catenin signaling, thereby enhancing TCF/LEF-driven gene expression in NSCLC [9]. We therefore hypothesized that the cluster perpetuates its own expression through the β-catenin/TCF4 axis. To validate this, we first established TCF4's role in cluster regulation. TCF4 overexpression markedly increased levels of miR-23a, miR-27a, and miR-24-2 **(Figure 6b)** and boosted promoter-driven luciferase activity **(Figure 6c).** EMSA confirmed direct TCF4 binding to the cluster promoter sequence containing TCF4 motifs, with binding strongly diminished by site mutation **(Figure 6d)**. These data demonstrate that TCF4 drives cluster miRNA expression via direct promoter interaction. We then assessed β-catenin's influence on TCF4-mediated cluster transcription. β-catenin overexpression enhanced TCF4 recruitment to the cluster promoter **(Figures 6e and 6f)**, increased promoter luciferase activity **(Figure 6g),** and elevated cluster miRNA levels **(Figure 6h).** Notably, the small-molecule inhibitor LF3, which disrupts β-catenin–TCF4 interaction, abolished β-catenin-induced cluster miRNA upregulation **(Figure 6i).** Collectively, these results show that the miR-23a/27a/24−2 cluster maintains its expression in NSCLC through a β-catenin/TCF4-dependent mechanism.

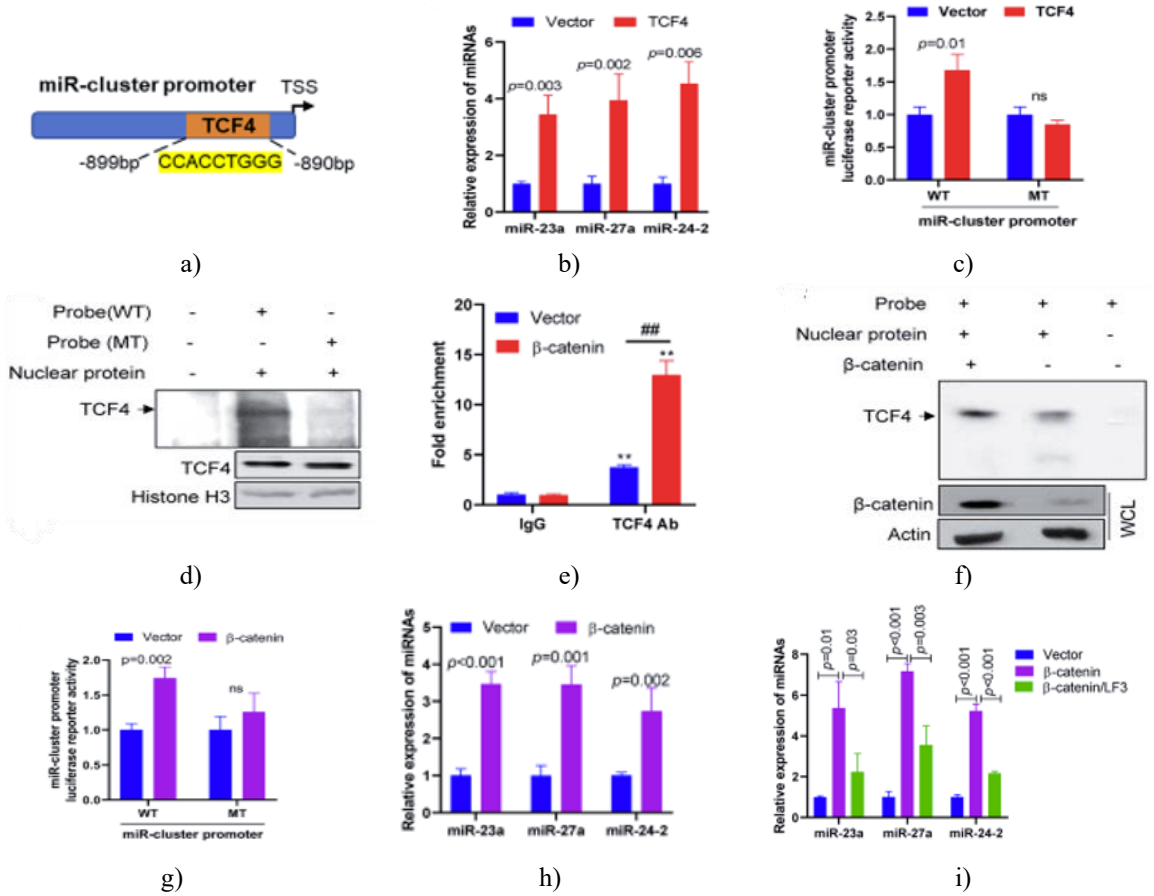

Figure 6. The miR-23a/27a/24−2 cluster sustains its own expression via the β-catenin/TCF4 pathway in NSCLC. (a) Predicted TCF4-binding sequences within the miR-23a/27a/24−2 cluster promoter region. (b) qRT-PCR demonstrating that TCF4 overexpression elevates levels of all miR-23a/27a/24−2 cluster miRNAs in 293T cells. (c) Luciferase reporter assay indicating that TCF4 overexpression boosts activity driven by the wild-type miR-23a/27a/24−2 cluster promoter in 293T cells. (d) EMSA confirming direct binding between

TCF4 and the miR-23a/27a/24−2 cluster promoter in 293T cells. (e) ChIP-qPCR results revealing that β-catenin overexpression enhances TCF4 recruitment to the miR-23a/27a/24−2 cluster promoter in 293T cells. , $p < 0.01$ versus Vector control (IgG); ##, $p < 0.01$ versus Vector control (TCF4 Ab). (f) EMSA demonstrating that β-catenin overexpression strengthens TCF4 binding to the miR-23a/27a/24−2 cluster promoter in 293T cells. (g) Luciferase reporter assay showing that β-catenin overexpression stimulates wild-type miR-23a/27a/24−2 cluster promoter-driven luciferase activity in 293T cells, without impacting the mutated promoter version. (h) qRT-PCR indicating that β-catenin overexpression raises expression of all miR-23a/27a/24−2 cluster miRNAs. (I) qRT-PCR showing that disrupting β-catenin–TCF4 interaction with 30 μM LF3 (6 h) prevents β-catenin-driven elevation of miR-23a/27a/24−2 cluster miRNAs in 293T cells. For (B-H), 293T cells were transfected with specified constructs for 72 h prior to analysis. Data represent mean ± SD. Significance by t-test (b, c, g, h) or one-way ANOVA with Duncan's multiple range test (e, i). miR-cluster, miR-23a/27a/24−2 cluster; ns, no significance; WT, wild type; MT, mutant; WCL, whole cell lysate.

Inhibiting the eIF3B pathway substantially boosts PD-1/PD-L1 blockade effectiveness in lung tumors exhibiting elevated miR-23a/27a/24−2 cluster miRNA levels

Since miR-23a/27a/24−2 cluster miRNAs alter key factors influencing PD-1/PD-L1 inhibitor response, we examined if their high levels confer resistance to this therapy. Consistent with expectations, cluster overexpression diminished tumor responsiveness to PD-L1 monoclonal antibody **(Figure 7a)** and curtailed CD8+ T cell infiltration in LLC-derived C57BL/6J mouse xenografts **(Figure 7b).**

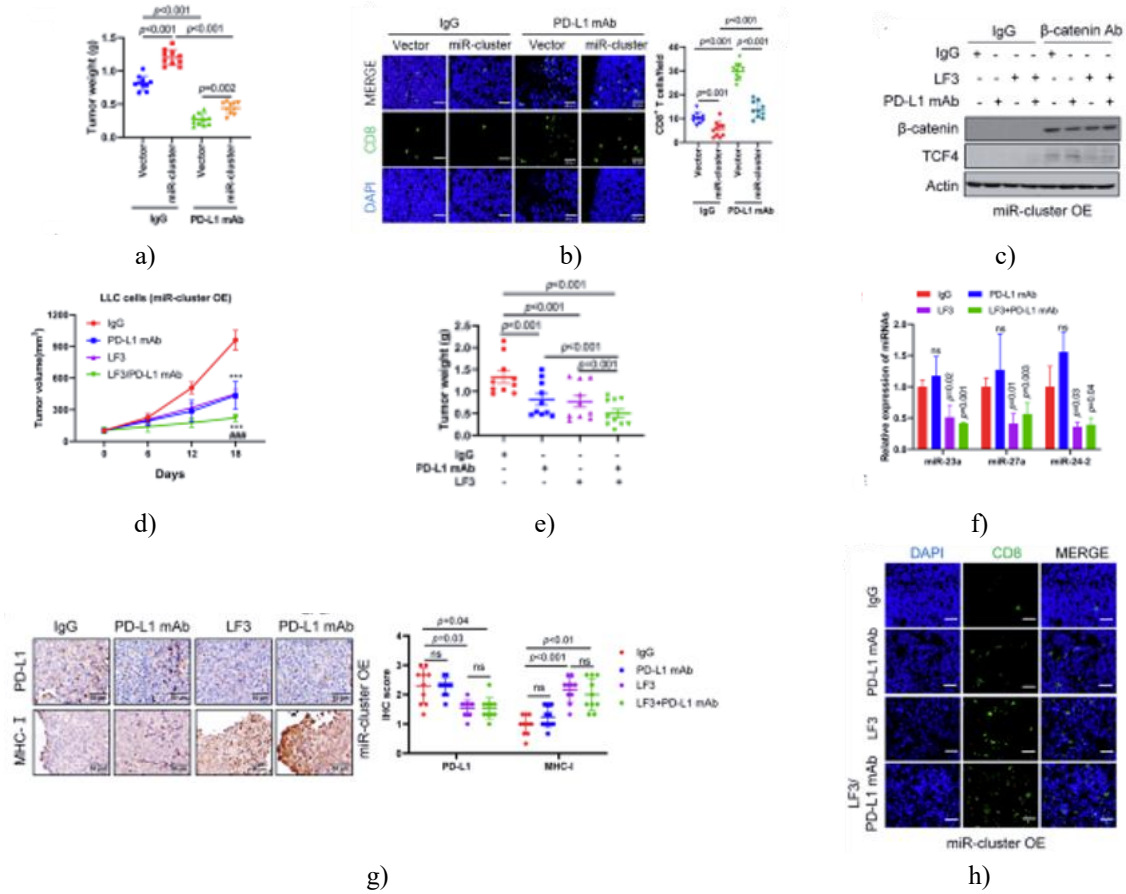

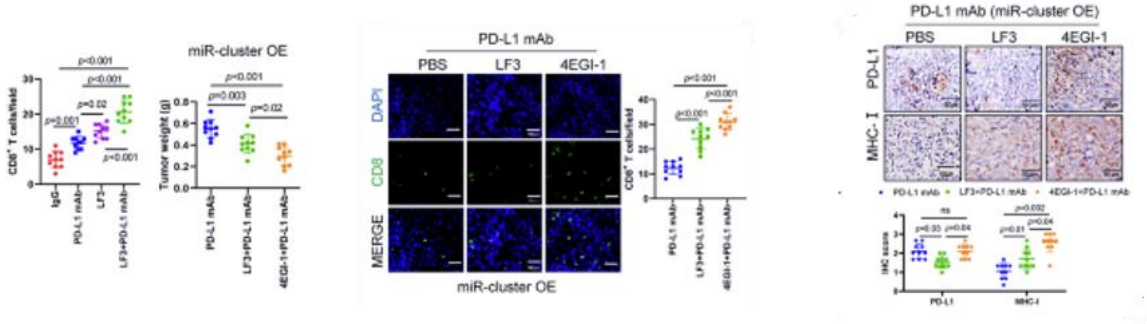

i) j) k)

Figure 7. Overexpression of the miR-23a/27a/24−2 cluster promotes resistance to PD-1/PD-L1 blockade in LLC-derived C57BL/6J xenografts, while eIF3B inhibition reverses this cluster-induced immune checkpoint blockade (ICB) resistance. (a) Tumor weights from vector-control or cluster-overexpressing LLC tumors in C57BL/6J mice treated with IgG or PD-L1 monoclonal antibody. (b) Representative immunofluorescence images of CD8+ T cells and quantification of infiltration (per 100 × 100 μm field; scale bar: 50 μm) in xenograft tumors from (a). (c) Co-IP demonstrating that LF3 markedly decreases β-catenin–TCF4 interaction in C57BL/6J xenograft tumors from (D). (d) Tumor growth curves, (e) final tumor weights, and (f) miR-23a/27a/24−2 cluster expression levels in C57BL/6J xenografts derived from cluster-overexpressing LLC cells. Tumors reached ~100 mm³ before treatment with IgG, PD-L1 mAb, LF3, or PD-L1 mAb plus LF3. (g) Representative IHC images and scores for PD-L1 and MHC-I in xenografts from indicated groups in (D) (scale bar: 50 μm). (H) Representative immunofluorescence for CD8+ T cells and infiltration counts (per 100 × 100 μm field) in tumors from indicated groups in (d) (scale bar: 50 μm). (i) Tumor weights, (j) representative immunofluorescence for CD8+ T cells (scale bar: 50 μm) with infiltration quantification (per 100 × 100 μm field), and (k) representative IHC images (scale bar: 50 μm) with scores for PD-L1 and MHC-I in cluster-high C57BL/6J xenografts treated as indicated. Cluster-high models were established with cluster-overexpressing LLC cells; treatments began at ~100 mm³ tumor volume, and tumors were harvested after 18 days for analyses (c-k). Each experimental group contained 10 mice. Data represent mean ± SD. Significance assessed by one-way ANOVA with Duncan's multiple range test (A, B, D, E, F, H, I, J) or Kruskal-Wallis with Dunn's test (g, k). miR-cluster, miR-23a/27a/24−2 cluster; miR-cluster OE, miR-23a/27a/24−2 cluster overexpression; PD-L1 mAb, PD-L1 monoclonal antibody; *, $p < 0.001$ versus IgG group; ###, $p < 0.001$ versus single-agent treatment group.

Prior research has established that activation of the β-catenin pathway [25] and the eIF3B/MHC-I axis [23] in tumors critically drives resistance to PD-1/PD-L1 inhibitors. Given that elevated miR-23a/27a/24−2 cluster expression fosters NSCLC resistance to PD-1/PD-L1 blockade—via self-sustainment through the β-catenin/TCF4 pathway and MHC-I suppression through eIF3B—we explored pharmacological interruption of these pathways to improve PD-1/PD-L1 blockade outcomes in cluster-high lung cancers. In vivo studies showed that disrupting β-catenin–TCF4 binding with LF3 **(Figure 7c)** substantially curtailed growth of cluster-high tumors relative to controls **(Figures 7d-7e)**. Strikingly, combining LF3 with PD-L1 monoclonal antibody exerted stronger tumor suppression than either agent alone in cluster-high lung tumors **(Figures 7d-7e).** LF3 also reduced cluster miRNA levels **(Figure 7f),** lowered PD-L1, and restored MHC-I expression **(Figure 7g).** The LF3 plus PD-L1 mAb regimen most effectively boosted CD8+ T cell tumor infiltration **(Figure 7h).** We then compared targeting β-catenin/TCF4 versus eIF3B alongside PD-1/PD-L1 blockade. Using 4EGI-1, which blocks eIF3B assembly in translation initiation and disrupts the MITF/eIF3B axis [23, 26], we found that eIF3B inhibition more potently augmented PD-L1 mAb efficacy in cluster-high lung cancers than β-catenin/TCF4 disruption with LF3 **(Figure 7i).** Furthermore, 4EGI-1 combined with PD-L1 mAb markedly enhanced CD8+ T cell infiltration **(Figure 7j)** and upregulated MHC-I without reducing the cluster-driven PD-L1 elevation **(Figure 7k).** Overall, these findings demonstrate that eIF3B targeting robustly improves PD-1/PD-L1 blockade effectiveness in lung cancers overexpressing the miR-23a/27a/24−2 cluster.

In the present work, we explored the molecular pathways through which miRNAs from the miR-23a/27a/24−2 cluster drive immune escape and resistance to PD-1/PD-L1 inhibition in NSCLC. Mounting evidence highlights PD-L1 [27] and MHC-I [28] as central regulators of antitumor immunity. PD-L1, displayed on tumor cell surfaces,

suppresses T cell activity by engaging PD-1 on T cells, making its aberrant overexpression a major route for tumor immune avoidance. Similarly, reduced MHC-I expression represents another critical escape mechanism. MHC-I presents peptide antigens on cell surfaces, enabling the immune system to identify and destroy aberrant cells [29]. When these peptides derive from tumor-associated antigens, antigen recognition activates CD8+ T cells, triggering cytotoxic elimination of malignant cells [29]. Regrettably, diminished or absent MHC-I occurs commonly across cancers, including lung cancer [30, 31], preventing T cell detection and permitting tumor survival [31]. Here, we showed that elevated miR-23a/27a/24−2 cluster miRNAs foster NSCLC immune evasion and PD-1/PD-L1 blockade resistance. Mechanistically, the cluster boosts PD-L1 by directly suppressing its negative regulator CBLB and lowers MHC-I by elevating the repressor eIF3B through direct targeting of MITF. Immune-suppressive roles for these cluster miRNAs have been noted in other malignancies. For instance, miR-27a was found to reduce MHC-I and CD8+ T cell infiltration in colorectal cancer [28]. Lin *et al*. observed miR-23a upregulation in CD8+ cytotoxic T lymphocytes, where its inhibition countered tumor-induced immunosuppression in lung cancer [32]. Additionally, heightened miR-23a and miR-27a in macrophages promote immune evasion via PD-L1 induction through the PTEN/PIK3 pathway in hepatocellular carcinoma [33] and breast cancer [34], respectively. Altogether, these reports reinforce that increased miR-23a/27a/24−2 cluster miRNAs facilitate tumor immune escape by elevating PD-L1 and diminishing MHC-I. Our investigation uncovers a previously unrecognized pathway for concurrent PD-L1 upregulation and MHC-I downregulation in NSCLC.

We also clarified how miR-23a/27a/24−2 cluster miRNAs sustain their elevated levels in NSCLC. Abnormal overexpression of this cluster occurs in roughly 50% of early-stage NSCLC cases and strongly associates with disease advancement [9], yet the underlying cause remained elusive. Here, we established that TCF4 directly binds the cluster promoter to enhance its transcription, with this binding augmented by β-catenin. Notably, our prior work demonstrated that these cluster miRNAs stimulate TCF/LEF-driven transcription by activating Wnt/β-catenin signaling through repression of its negative regulators in NSCLC [9]. Together, these observations indicate a positive feedback loop wherein the miR-23a/27a/24−2 cluster perpetuates its own expression via the β-catenin/TCF4 pathway in NSCLC. Interrupting this loop could thus offer a therapeutic avenue for cluster-high NSCLC. Indeed, our earlier findings showed that cluster knockdown or β-catenin silencing curbs tumor progression in such cases [9].

Lastly, we introduce an innovative treatment approach for NSCLC exhibiting high miR-23a/27a/24−2 cluster levels. Our data link the cluster to activation of β-catenin signaling [9] and the eIF3B axis, both implicated in PD-1/PD-L1 blockade resistance [23, 35]. We found that inhibiting either the β-catenin/TCF4 interaction or the eIF3B pathway markedly improves PD-L1 monoclonal antibody efficacy. Strikingly, eIF3B inhibition proved superior to β-catenin/TCF4 blockade. This difference likely arises from distinct effects on PD-L1 and MHC-I. Clinical evidence ties PD-1/PD-L1 blockade success to tumor PD-L1 levels [36, 37], and Zhang *et al*. showed that boosting PD-L1 can amplify therapeutic responses [38]. In our models, β-catenin/TCF4 inhibition restored MHC-I but reduced PD-L1, whereas eIF3B blockade preserved cluster-induced PD-L1 elevation while strongly upregulating MHC-I.

Conclusion

Overall, miR-23a/27a/24−2 cluster miRNAs sustain their abundance in NSCLC by engaging the β-catenin/TCF4 pathway. Elevated cluster expression raises PD-L1 via CBLB suppression and lowers MHC-I by increasing eIF3B through MITF targeting **(Figure 8a).** Moreover, this work offers a new therapeutic paradigm: eIF3B inhibition potently sensitizes cluster-high lung cancers to PD-1/PD-L1 blockade by recovering MHC-I while retaining the cluster-driven high PD-L1 state **(Figure 8b).**

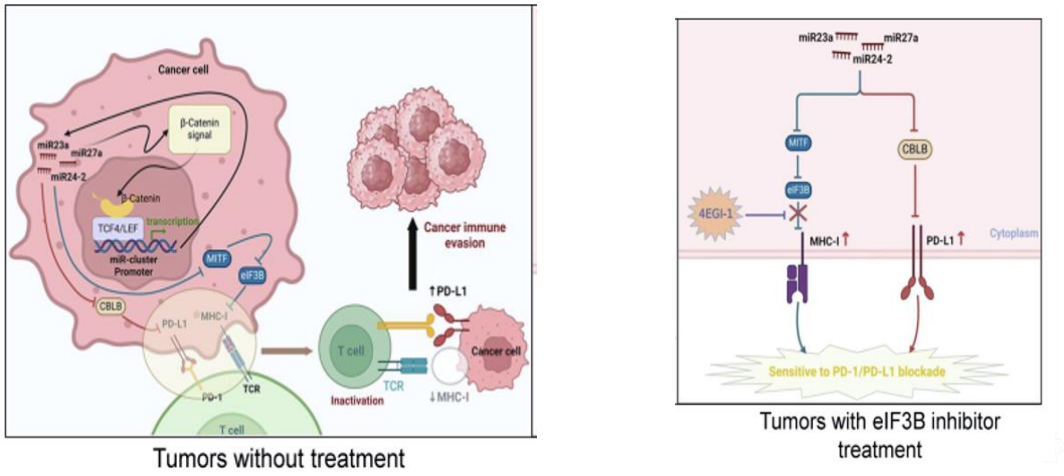

Figure 8. Schematic models illustrating how miR-23a/27a/24−2 cluster miRNAs perpetuate their expression and drive tumor immune evasion (a), and how eIF3B targeting renders cluster-high tumors responsive to PD-1/PD-L1 inhibition (b).

Acknowledgments: None

Conflict of Interest: None

Financial Support: None

Ethics Statement: None

References

1. Bray F, Laversanne M, Sung HYA, Ferlay J, Siegel RL, Soerjomataram I, Jemal A. Global cancer statistics 2022: GLOBOCAN estimates of incidence and mortality worldwide for 36 cancers in 185 countries. Ca-Cancer J Clin. 2024;74(3):229–63.
2. Cronin KA, Lake AJ, Scott S, Sherman RL, Noone AM, Howlader N, Henley SJ, Anderson RN, Firth AU, Ma JM et al. Annual Report to the Nation on the Status of Cancer, part I: National cancer statistics. Cancer-Am Cancer Soc. 2018;124(13):2785–2800.
3. Zavitsanou AM, Pillai R, Hao Y, Wu WL, Bartnicki E, Karakousi T, Rajalingam S, Herrera A, Karatza A, Rashidfarrokhi A, et al. KEAP1 mutation in lung adenocarcinoma promotes immune evasion and immunotherapy resistance. Cell Rep. 2023;42(11):113295.
4. Vinay DS, Ryan EP, Pawelec G, Talib WH, Stagg J, Elkord E, Lichtor T, Decker WK, Whelan RL, Kumara HMCS, et al. Immune evasion in cancer: mechanistic basis and therapeutic strategies. Semin Cancer Biol. 2015;35:S185–98.
5. Cable J, Greenbaum B, Pe'er D, Bollard CM, Bruni S, Griffin ME, Allison JP, Wu CJ, Subudhi SK, Mardis ER et al. Frontiers in cancer immunotherapy-a symposium report. Ann Ny Acad Sci: 2021, 1489(1):30–47.
6. Sharma P, Hu-Lieskovan S, Wargo JA, Ribas A. Primary, adaptive, and Acquired Resistance to Cancer Immunotherapy. Cell. 2017;168(4):707–23.
7. Cioffi M, Trabulo SM, Vallespinos M, Raj D, Kheir TB, Lin ML, Begum J, Baker AM, Amgheib A, Saif J et al. The miR-25-93-106b cluster regulates tumor metastasis and immune evasion via modulation of CXCL12 and PD-L1. Oncotarget. 2017;8(13):21609–21625.
8. Kundu ST, Rodriguez BL, Gibson LA, Warner AN, Perez MG, Bajaj R, Fradette JJ, Class CA, Solis LM, Alvarez FRR, et al. The microRNA-183/96/182 cluster inhibits lung cancer progression and metastasis by inducing an interleukin-2-mediated antitumor CD8 cytotoxic T-cell response. Gene Dev. 2022;36(9–10):582–600.
9. Fan XQ, Tao SL, Li Q, Deng B, Tan QY, Jin H. The miR-23a/27a/24 – 2 cluster promotes postoperative progression of early-stage non-small cell lung cancer. Mol Ther-Oncolytics. 2022;24:205–17.

10. Muto S, Enta A, Maruya Y, Inomata S, Yamaguchi H, Mine H, Takagi H, Ozaki Y, Watanabe M, Inoue T, et al. Wnt/β-Catenin signaling and resistance to Immune Checkpoint inhibitors: from non-small-cell lung Cancer to other cancers. Biomedicines. 2023;11(1):190.
11. Chandran PA, Keller A, Weinmann L, Seida AA, Braun M, Andreev K, Fischer B, Horn E, Schwinn S, Junker M, et al. The TGF-β-inducible miR-23a cluster attenuates IFN-γ levels and antigen-specific cytotoxicity in human CD8 T cells. J Leukoc Biol. 2014;96(4):633–45.
12. Li Q, Zhou ZW, Lu J, Luo H, Wang SN, Peng Y, Deng MS, Song GB, Wang JM, Wei X, et al. PD-L1P146R is prognostic and a negative predictor of response to immunotherapy in gastric cancer. Mol Ther. 2022;30(2):621–31.
13. Shang S, Yang YW, Chen F, Yu L, Shen SH, Li K, Cui B, Lv XX, Zhang C, Yang C, et al. TRIB3 reduces CD8 T cell infiltration and induces immune evasion by repressing the STAT1-CXCL10 axis in colorectal cancer. Sci Transl Med. 2022;14(626):eabf0992.
14. Li Q, Zhou ZW, Duan W, Qian CY, Wang SN, Deng MS, Zi D, Wang JM, Mao CY, Song GB, et al. Inhibiting the redox function of APE1 suppresses cervical cancer metastasis via disengagement of ZEB1 from E-cadherin in EMT. J Exp Clin Canc Res. 2021;40(1):220.
15. Nuovo GJ. In situ detection of microRNAs in paraffin embedded, Formalin fixed tissues and the co-localization of their putative targets. Methods. 2010;52(4):307–15.
16. Guo ZY, Hardin H, Montemayor-Garcia C, Asioli S, Righi A, Maletta F, Sapino A, Lloyd RV. In situ hybridization analysis of miR-146b-5p and miR-21 in thyroid nodules: diagnostic implications. Endocr Pathol. 2015;26(2):157–63.
17. Li JW, Jiang HM, Lv ZY, Sun ZY, Cheng CQ, Tan GH, Wang MC, Liu AL, Sun H, Guo H, et al. Articular fibrocartilage-targeted therapy by microtubule stabilization. Sci Adv. 2022;8(46):eabn8420.
18. Dai FQ, Li CR, Fan XQ, Tan L, Wang RT, Jin H. Mir-150-5p inhibits non-small-cell Lung Cancer Metastasis and recurrence by targeting HMGA2 and β-Catenin signaling. Mol Ther-Nucl Acids. 2019;16:675–85.
19. Zhang Q, Liu W, Zhang HM, Xie GY, Miao YR, Xia MX, Guo AY. hTFtarget: a comprehensive database for regulations of human transcription factors and their targets. Genom Proteom Bioinf. 2020;18(2):120–8.
20. Vlachos IS, Zagganas K, Paraskevopoulou MD, Georgakilas G, Karagkouni D, Vergoulis T, Dalamagas T, Hatzigeorgiou AG. DIANA-miRPath v3.0: deciphering microRNA function with experimental support. Nucleic Acids Res. 2015;43(W1):W460–6.
21. Liu ZC, Wang TT, She YL, Wu KQ, Gu SR, Li L, Dong CL, Chen C, Zhou YX. N-methyladenosine-modified circIGF2BP3 inhibits CD8 T-cell responses to facilitate tumor immune evasion by promoting the deubiquitination of PD-L1 in non-small cell lung cancer. Mol Cancer. 2021;20(1):105.
22. Wang S, Xu L, Che XF, Li C, Xu L, Hou KZ, Fan YB, Wen T, Qu XJ, Liu YP. E3 ubiquitin ligases Cbl-b and c-Cbl downregulate PD-L1 in wild-type non-small cell lung cancer. Febs Lett. 2018;592(4):621–30.
23. Santasusagna S, Zhu S, Jawalagatti V, Carceles-Cordon M, Ertel A, Garcia-Longarte S, Song WM, Fujiwara N, Li P, Mendizabal I, et al. Master transcription factor reprogramming unleashes selective translation promoting Castration Resistance and Immune Evasion in Lethal prostate Cancer. Cancer Discov. 2023;13(12):2584–609.
24. Rambow F, Bechadergue A, Luciani F, Gros G, Domingues M, Bonaventure J, Meurice G, Marine JC, Larue L. Regulation of Melanoma Progression through the TCF4/miR-125b/NEDD9 Cascade. J Invest Dermatol. 2016;136(6):1229–37.
25. de Galarreta MR, Bresnahan E, Molina-Sánchez P, Lindblad KE, Maier B, Sia D, Puigvehi M, Miguela V, Casanova-Acebes M, Dhainaut M, et al. β-Catenin activation promotes Immune escape and resistance to Anti-PD-1 therapy in Hepatocellular Carcinoma. Cancer Discov. 2019;9(8):1124–41.
26. Moerke NJ, Aktas H, Chen H, Cantel S, Reibarkh MY, Fahmy A, Gross JD, Degterev A, Yuan JY, Chorev M, et al. Small-molecule inhibition of the interaction between the translation initiation factors eIF4E and eIF4G. Cell. 2007;128(2):257–67.
27. Wang J, Ge JS, Wang YA, Xiong F, Guo JY, Jiang XJ, Zhang LS, Deng XY, Gong ZJ, Zhang SS, et al. EBV miRNAs BART11 and BART17-3p promote immune escape through the enhancer-mediated transcription of PD-L1. Nat Commun. 2022;13(1):866.
28. Colangelo T, Polcaro G, Ziccardi P, Pucci B, Muccillo L, Galgani M, Fucci A, Milone MR, Budillon A, Santopaolo M, et al. Proteomic screening identifies calreticulin as a miR-27a direct target repressing MHC class I cell surface exposure in colorectal cancer. Cell Death Dis. 2016;7(2):e2120.

29. Wu XY, Li TH, Jiang R, Yang X, Guo HQ, Yang R. Targeting MHC-I molecules for cancer: function, mechanism, and therapeutic prospects. Mol Cancer. 2023;22(1):194.
30. Korkolopoulou P, Kaklamanis L, Pezzella F, Harris AL, Gatter KC. Loss of antigen-presenting molecules (MHC class I and TAP-1) in lung cancer. Brit J Cancer. 1996;73(2):148–53.
31. Dhatchinamoorthy K, Colbert JD, Rock KL. Cancer Immune Evasion through loss of MHC Class I Antigen Presentation. Front Immunol. 2021;12:636568.
32. Lin R, Chen L, Chen G, Hu CY, Jiang S, Sevilla J, Wan Y, Sampson JH, Zhu B, Li QJ. Targeting miR-23a in CD8 cytotoxic T lymphocytes prevents tumor-dependent immunosuppression. J Clin Invest. 2014;124(12):5352–67.
33. Liu JT, Fan LL, Yu HQ, Zhang J, He Y, Feng DC, Wang F, Li XQ, Liu QQ, Li YH, et al. Endoplasmic reticulum stress causes Liver Cancer cells to Release Exosomal miR-23a-3p and Up-regulate programmed death Ligand 1 expression in macrophages. Hepatology. 2019;70(1):241–58.
34. Yao XL, Tu Y, Xu YL, Guo YY, Yao F, Zhang XH. Endoplasmic reticulum stress-induced exosomal miR-27a-3p promotes immune escape in breast cancer via regulating PD-L1 expression in macrophages. J Cell Mol Med. 2020;24(17):9560–73.
35. Luke JJ, Bao RY, Sweis RF, Spranger S, Gajewski TF. WNT/β-catenin pathway activation correlates with Immune Exclusion across Human cancers. Clin Cancer Res. 2019;25(10):3074–83.
36. Herbst RS, Soria JC, Kowanetz M, Fine GD, Hamid O, Gordon MS, Sosman JA, McDermott DF, Powderly JD, Gettinger SN, et al. Predictive correlates of response to the anti-PD-L1 antibody MPDL3280A in cancer patients. Nature. 2014;515(7528):563–7.
37. Iwai Y, Ishida M, Tanaka Y, Okazaki T, Honjo T, Minato N. Involvement of PD-L1 on tumor cells in the escape from host immune system and tumor immunotherapy by PD-L1 blockade. P Natl Acad Sci USA. 2002;99(19):12293–7.
38. Zhang JF, Bu X, Wang HZ, Zhu YS, Geng Y, Nihira NT, Tan YY, Ci YP, Wu F, Dai XP, et al. Cyclin D-CDK4 kinase destabilizes PD-L1 via cullin 3-SPOP to control cancer immune surveillance. Nature. 2018;553(7686):91–5.